Earth and Planetary Science Letters 461 (2017) 1–7

Contents lists available at ScienceDirect

Earth and Planetary Science Letters

www.elsevier.com/locate/epsl

Gutenberg–Richter law for deep earthquakes revisited: A dual-mechanism hypothesis

Zhongwen Zhan

Seismological Laboratory, Division of Geological and Planetary Sciences, California Institute of Technology, 1200 E. California Boulevard, Pasadena, CA 91125, USA

ARTICLE INFO

Article history:
Received 26 August 2016
Received in revised form 26 November 2016
Accepted 22 December 2016
Available online xxxx
Editor: B. Buffett

Keywords:
deep earthquakes
Gutenberg–Richter law
frequency–magnitude distribution

ABSTRACT

Deep earthquake b values appear to vary with slab thermal state and earthquake magnitude. The physical reason for the variations and the relation with deep rupture mechanisms are still unclear. Here I confirm the spatial variations of b value and the dependence on slab temperature using about 40 yr of data from the Global Centroid Moment Tensor catalog. A new bimodal pattern is observed for the 500–700 km depth range: b is close to 1 in the cold Tonga slab, while in warmer slabs (e.g., South America, Japan–Kuril, Izu–Bonin–Mariana), b is close to 0.5 for intermediate magnitudes (M_w5.3–6.5) and increases to ∼1 for large magnitudes ($M_w > 6.5$). To explain these observations, I propose a dual-mechanism hypothesis in which deep earthquakes nucleate only within the metastable olivine wedge (MOW), but can rupture outside MOW by a different mechanism. The fractal dimension of earthquake size distribution changes from 2 to 1 as the thermally controlled MOW thickness decreases, and back to 2 as the mechanism outside MOW dominates.

1. Introduction

Deep earthquakes follow the Gutenberg–Richter (G–R) law, $\log_{10} N = a - bM$. One remarkable observation about deep earthquakes (depth > 300 km) is that the b values vary significantly among different subduction zones (Giardini, 1988; Pacheco et al., 1992; Okal and Kirby, 1995; Wiens and Gilbert, 1996). For example, Tonga subduction zone ($b \gtrsim 1$) produced 70% of the global deep earthquakes above $M4$, but only about a third of the events above M7. In contrast, South American subduction zone, with a small b, contributed about a similar number of $M > 7$ events as Tonga, with only 3% of deep seismicity above $M4$. Wiens and Gilbert (1996) showed that deep earthquake b values appear to be temperature dependent, which suggests thermally controlled rupture mechanisms (e.g., shear melting). Furthermore, changes in b value at certain magnitude (i.e., kinks) for deep earthquakes have been reported and interpreted by seismogenic width saturation, similarly as for crustal earthquakes (Pacheco et al., 1992; Okal and Kirby, 1995). However, in the 1990s, the sample size for large magnitudes was small and the kinks were not statistically convincing.

The aforementioned studies were along with the intense discussions about the G–R law of crustal earthquakes in the 1990s (Rundle, 1989; Pacheco et al., 1992; Romanowicz and Rundle, 1993; Scholz, 1997). Since then, while data have nearly doubled with 20 more years of deep seismicity, there has not been a thorough revisit. Meanwhile, detailed studies of individual large deep earthquakes in the last two decades also provide us new insights about deep earthquake rupture processes. In this paper, I revisit the G–R law for deep earthquakes and propose a dual-mechanism hypothesis to explain the spatial and magnitude dependences of b values. I use the Global Centroid Moment Tensor (GCMT) catalog (Dziewonski et al., 1981; Ekström et al., 2012) from 1977 to 2016 to ensure consistent moment magnitude estimates, instead of combining different types of magnitude (e.g., mb or Ms). I divide the global deep earthquake distribution into six regions (Fig. 1): South America (SA), Tonga, Japan–Kuril (JK), Izu–Bonin–Mariana (IBM), Philippine (PH), and Indonesia (Indo), each of which feature relatively uniform tectonics but still have enough samples for robust statistics. As references, I also analyze intermediate-depth earthquakes (70–300 km) in the same regions (blue dots in Fig. 1). I use the traditional divide of 300-km depth between intermediate-depth and deep earthquakes, but have also verified that other choices (e.g., 400 km) do not change the general observations. This is probably due to the relatively low seismicity in the 300–400 km depth range globally.

E-mail address: zwzhan@gps.caltech.edu.

http://dx.doi.org/10.1016/j.epsl.2016.12.030
0012-821X/

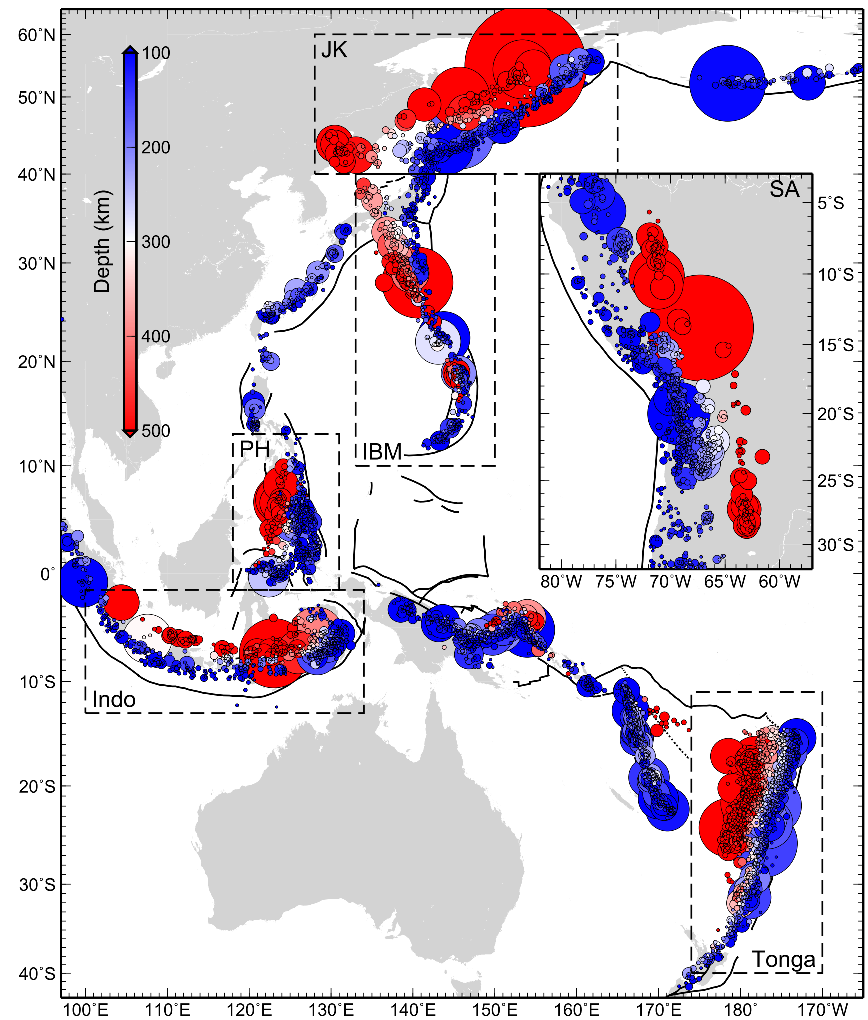

Fig. 1. Distribution of deep (red dots) and intermediate-depth (blue dots) earthquakes analyzed in this study. Dot sizes are proportional to rupture dimensions assuming a constant strain drop. Deep earthquakes are divided into six regions as defined by the dashed rectangles. (For interpretation of the references to color in this figure legend, the reader is referred to the web version of this article.)

2. Regional variations of *b* value for intermediate magnitudes

Fig. 2 shows the frequency–magnitude distributions, $N(M_w)$, defined as the cumulative number of events with magnitude larger than M_w, for the six regions and three different depth ranges. $N(M_w)$ in the intermediate depth range (green diamonds) show similar slopes for all six regions, while $N(M_w)$ in the 300–700 km (blue squares) and 500–700 km (red dots) depth ranges show more variations. For example, deep and intermediate-depth events in Tonga have about the same slopes (Fig. 2f), while the slope for deep events in SA is much smaller than the slope for intermediate-depth events (Fig. 2a).

To estimate the *b* values quantitatively, I conduct robust linear fitting of $N(M_w)$ using the Huber norm (Huber, 1973; Lin et al., 2007; Huang and Beroza, 2015), between M_w5.3, chosen to be slightly above GCMT's detection threshold for deep earthquakes, and $M_w^{\max}$ for which at least 10 events are present in a given region (larger symbols in Fig. 2). Fitting $N(M_w)$ for M_w above $M_w^{\max}$ may become unstable due to the small (<10) sample sizes. Finally I do a bootstrapping with 10,000 resamples to estimate the 95% confidence interval of *b* value. Fig. 3 shows the measured *b* values as a function of the average thermal parameters for the six regions, taken from Wiens and Gilbert (1996) and Frohlich (2006). *b* values of deep earthquakes (red dots and blue squares) are strongly temperature dependent, high in cold slabs and low in warm slabs. Meanwhile, intermediate-depth events (green diamonds in Fig. 3) do not show such a trend. Except the slightly larger *b* value for the Indonesia region, all the other regions have *b* values between 0.9 and 1.1 for intermediate depths (70–300 km). This clear lack of correlation between *b* values of deep and intermediate-depth earthquakes suggests that the cause of the spatial variations in deep earthquake *b* values is probably not inherited from shallower depths (e.g., fault roughness/length distributions).

There are two new observations. (1) The *b* values decrease with depth below 300 km at least in some slabs. For the JK and IBM regions, the drops of *b* values from 300–700 km to 500–700 km are statistically significant. This may be another form of temperature dependence as slabs warm up. (2) More importantly, in the 500–700 km depth range (solid red dots in Fig. 3), *b* values of the six regions show a sharp transition over only 2000 km of slab thermal parameters: *b* values in the four warmer slabs (SA, PH, JK, and IBM) are close to 0.5 without much variation over the wide range of thermal parameters, while the *b* value rises to about 1.1 in the coldest slab (Tonga). The only transition in between, Indonesian subduction zone, is related to varying thermal parameters within the region from west to east (Frohlich, 2006). If I isolate the warmer western half of the Indonesian region, the *b* value is close to 0.5, with a larger uncertainty due to a smaller sample size (W-Indo in Fig. 3).